

# Bulk and Interfacial Studies of a New and Versatile Semifluorinated Lyotropic Liquid Crystalline Polymer

R. Traiphol,<sup>†</sup> H. Shah,<sup>†,‡</sup> D. W. Smith, Jr.,<sup>\*,†,§</sup> and D. Perahia<sup>\*,†,§</sup>

Department of Chemistry, and Material Science and Engineering Program, Clemson University, Clemson, South Carolina 29634-0973

Received October 17, 2000; Revised Manuscript Received February 19, 2001

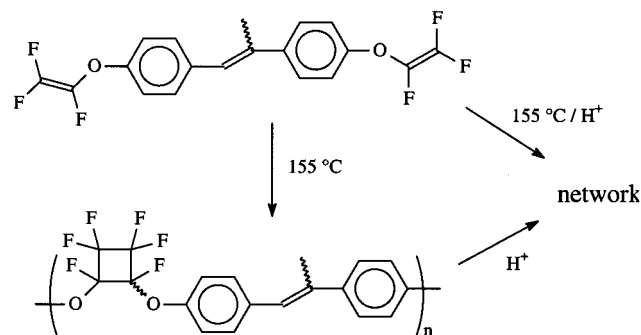
**ABSTRACT:** This study introduces the phase diagram and interfacial characteristics of a novel lyotropic polymeric liquid crystal. The polymer consists of an  $\alpha$ -methylstilbene mesogenic group bridged by a low interfacial energy perfluorocyclobutyl ring via flexible aryl ether linkages. The polymer, obtained by thermal cyclopolymerization of trifluorovinyl ether monomers, forms lyotropic lamellar mesophases over a wide range of temperatures and molecular weights. Mesophase behavior probed by optical microscopy, AFM, NMR, and X-ray scattering is detailed. The lamellae consist of longer chains, immersed in a solvent of smaller chains. The interfacial characteristics of these lyomesophases are affected by the low surface energy moiety. At the interface with glass, homeotropic alignment is observed. When cast into thin films, an additional periodicity on the nanometer scale has been detected. Thin films consist of spontaneously oriented bundles with characteristic length scale on 50 nm.

## Introduction

This study introduces the phase diagram and interfacial characteristics of a novel lyotropic polymeric liquid crystal (PLC). The linear polymer shown in Scheme 1 consists of an  $\alpha$ -methylstilbene mesogenic group, bridged by a perfluorocyclobutyl (PFCB) ring via a flexible ether linkage.<sup>1,2</sup> We recently reported that this polymer exhibits mesomorphic properties for a degree of polymerization (DP) higher than ca. 10.<sup>1</sup> Polymer is obtained by thermal step-growth cyclopolymerization of the corresponding bis(trifluorovinyl) ether monomer, thus the polydispersity approaches 2 for linear polymerization and between 2 and 3 for the branched polymers (Scheme 1). While the mesophase consists of a mixture of oligomer sizes, well-defined physical properties and discrete phase transitions have been observed. This is a characteristic response of lyotropic liquid crystals (LC), where mesogenic molecules are immersed in solvents to form an ordered mesophase.

The uniqueness of the lyotropic system under consideration lies in the semifluorinated nature of the polymeric liquid crystal and in the synthetic pathway, which permit control of DP, branching and ultimate branched of the PLC.<sup>1</sup> The introduction of fluorinated groups on the backbone of a LC changes the intermolecular interactions, hence affecting the ordering of the molecule and other physical properties. This change is a direct result of the low interfacial energy of fluorinated linkages. The surface energies or the surface tension  $\gamma$ , can be expressed in terms of the density of the polymer  $\rho$ , and the Maclond exponent  $\beta$ , which is between 3 and 4.5 for polymers,<sup>3</sup>  $\gamma = \gamma^0 \rho^\beta$  (where  $\gamma^0$  is a constant, which depends mostly on the surface chemical and physical structure). For organic surfaces, it has been established that the surface energy decreases with increasing

**Scheme 1. Cyclopolymerization of Bis(trifluorovinyl) Ether (TFVE) Monomer (1) Containing an  $\alpha$ -Methylstilbene Mesogenic Group<sup>a</sup>**



<sup>a</sup> By heating above 150 °C under N<sub>2</sub> atmosphere, it yields branched or linear polymers depending on pH.

fluorine content in the following order: CH<sub>2</sub> > CH<sub>3</sub> > CF<sub>2</sub> > CF<sub>3</sub> (36:30:23:15 dyn/cm respectively).<sup>4</sup> In addition to the effects on interfacial energies, increasing fluorine content has also proven to increase the thermal and chemical stability of most molecules.<sup>5</sup>

Currently liquid crystals are used in LC displays and electrooptic devices where well-controlled orientational ordering and interfacial interactions together with thermal and chemical stability are required. The potential of fluorinated LCs to enhance their performance in optical applications has resulted in intensive synthetic effort to generate new fluorinated small and polymeric liquid crystals.<sup>5–18</sup> In particular, approaches to utilize the incompatibility between hydrogen and fluorine to form segregated amphiphile-like molecules that exhibit mesomorphic behavior have been established.<sup>7,14</sup> This segregation has been a driving force for orientation on molecules, similar to the effects observed in diblock copolymers.<sup>19</sup> Ober et al. have shown in several comprehensive studies that this segregation is a driving force not only for the formation of organized LC phases, but it also controls the interfacial characteristics of thin films made by fluorine containing liquid crystalline materials.<sup>6</sup>

\* Authors for correspondence.

<sup>†</sup> Department of Chemistry, Clemson University.

<sup>‡</sup>Current address: Optical Coatings Laboratory/JDS Uniphase Corp., 2789 Northpoint Parkway, Santa Rosa, CA 95407-7397.

<sup>§</sup> Material Science and Engineering Program, Clemson University.

**Table 1. Molecular Weight as a Function of Polymerization Time (*t*) Obtained from GPC Using Standard Polystyrene**

<i>t</i> (min)	branched		<i>t</i> (min)	linear	
	$M_n \times 10^{-3}$ g/mol	$M_w/M_n$		$M_n \times 10^{-3}$ g/mol	$M_w/M_n$
200	1.49	1.43	150	1.90	1.40
250	2.24	1.74	300	2.86	1.62
300	3.16	2.27	540	4.19	1.80
330	3.56	2.58	1050	7.22	2.07
370	3.97	5.64	1860	12.19	2.65
410	5.45	19.79			
820	insoluble				

As mentioned above PLCs are widely used in LCD display technology. One of the major challenges in this technology is to obtain a LC layer that would be oriented by the surface but will simultaneously exhibit a fast and steep electrooptical response. The control over surface energy achieved by the introduction of fluorine allows the manipulation of both the surface alignment and surface anchoring.<sup>12</sup> Fluorinated polymers have also been used as surface alignment layers. Depending on the preparation method, either homogeneous or homeotropic layers can be obtained.<sup>18,20–23</sup>

We have recently developed a new system based on the bis(trifluorovinyl) ether monomer shown in Scheme 1. When heated, this particular mesogenic monomer undergoes cyclopolymerization to form perfluorocyclobutane (PFCB) linear, branched, or network polymer depending on conditions.<sup>1</sup> We have shown that linear and branched structures exhibit lyotropic behavior. The potential of the network as an orienting layer is also currently being explored. Here we present the phase diagrams for the lyotropic mesophases of both linear and branched polymers, followed by the dynamics of the molecules in the mesophase together with further interfacial characteristics.

## Experimental Section

4,4'-Bis(trifluorovinyl)oxy- $\alpha$ -methylstilbene monomer (**1**) was synthesized as described recently in ref 1. Polymerization was accomplished by heating the neat monomers at 155–160 °C. A series of polydispersed polymers with variable chain lengths were obtained by heating for different periods of time. The list of the studied oligomers is given in Table 1.

The molecular weights of the PLCs were determined by gel permeation chromatography (GPC) Waters 2690 Alliance system in conjunction with 2410 refractive index and 996 photodiode array detectors. The phase boundaries and some surface characteristics were obtained from polarized optical microscopy (POM) (Jame Swift microscope fitted with Mettler FH-82 hot stage). DSC measurements were carried out on a Mettler-Toledo DSC820 system.<sup>24</sup>

The ordering of the system was studied using NMR measurements on <sup>2</sup>H, <sup>1</sup>H, and <sup>19</sup>F (Bruker AC200 spectrometer) at 30, 200, and 188 MHz, respectively. The NMR is equipped with a variable-temperature unit. For <sup>2</sup>H NMR experiment, ~1 wt % of cyclohexane-*d*<sub>12</sub> (Cambridge Isotope Laboratories) was added to monomers prior to the polymerization.<sup>25,26</sup>

Further structural information was obtained by X-ray measurements carried out on a Sintag XDS2000 equipped with a Cu tube ( $\lambda = 1.54$  Å) operating at 40 kV and 20 mA for the small angle (SAXS) region and at 40 kV and 30 mA for the wide-angle range. The beam has a rectangular shape and is 20 mm  $\times$  0.8 mm (width at half-maximum). The geometry of a  $\theta$ - $\theta$  instrument implies that the experiments are carried out in a reflection mode; thus, the data presented are scattering results on top of a reflectivity curve. This becomes most significant for the SAXS measurements where any correlation

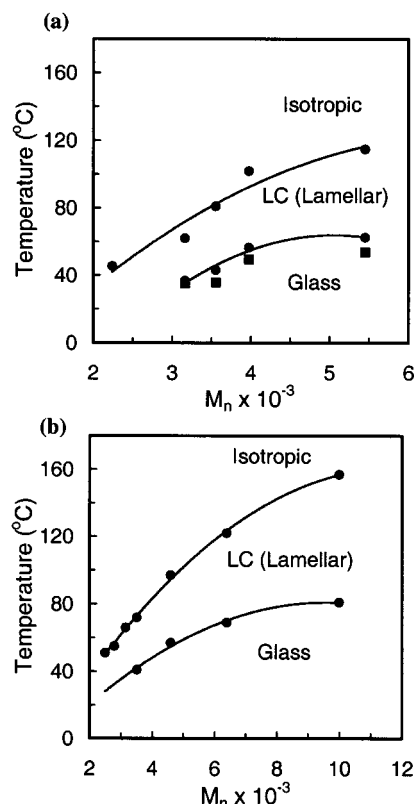


**Figure 1.** Phase diagrams of (a) branched (b) linear polymer obtained from (●) polarized optical microscopy and (■) DSC. The lamellar structure of LC was revealed by SAXS (see text). The lines are obtained by exponential fits.

lines are detected on top of the reflectivity and on the shoulder of the main beam. The Sintag is not equipped with a monitor; thus, the SAXS data are measured and presented as raw data on top of the main beam profile. Since the system does not have a monitor, any attempt to normalize to background in this case introduces further distortion. Therefore, an error of about 5% has to be associated with the SAXS data. Both background and empty cell measurements accompanied every sample measurement. The SAXS data provide information on long range order in the system.

AFM measurements have been carried out on a digital multimode AFM in tapping mode. Olympus cantilevers, with a spring constant of 42 N/m, resonating at 300 kHz, have been used for all measurements. The strength of the tapping has been varied to meet the needs of the specific sample and will be indicated in the captions of the corresponding figures. Samples were prepared by dropping a dilute solution of the polymer in toluene (~1 wt %) on a microscope cover slide and allowing evaporation under clean atmosphere.

## Results and Discussion

**Phase Diagram.** The thermal polymerization of monomer (**1**) resulted in linear, branched, and network polymers,<sup>1</sup> depending on the pH during polymerization. The ability to control the polymerization mechanism is of unique advantage since it allows controlling the architecture and hence the properties of the LC. The phase diagrams of the linear and branched systems, as derived from polarized optical microscopy, differential scanning calorimetry (DSC), and X-ray scattering, are shown in Figure 1, parts a and b. Upon cooling the isotropic liquid of both linear and branched polymers, a sharp, first-order phase transition into a lamellar mesophase has been observed. The mesomorphic range of the linear system is significantly larger than that for

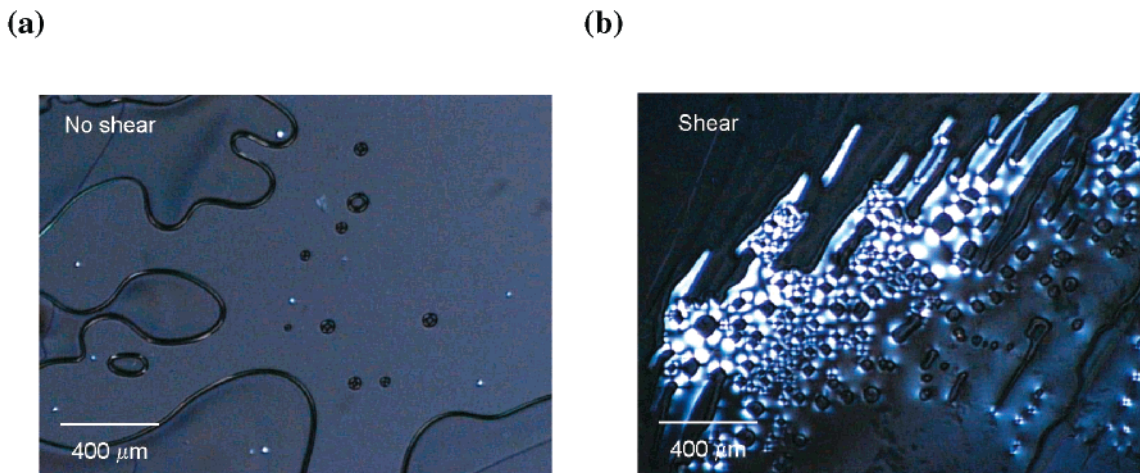


**Figure 2.** Polarized optical microscope images of branched oligomers ( $M_n = 2240$ ,  $M_n/M_w = 1.74$ ) at room temperature: (a) A static image without shear. (b) Dynamic image of the same sample presented in a sheared by sliding the top cover for about 2 mm without normal load. Similar texture was observed on linear polymer.

the branched PLC. All experiments have clearly shown that the system exhibits long-range orientational ordering, which is a characteristic of a liquid crystalline system. The polymerization results in a mixture of oligomers with polydispersity of  $\sim 2$ , resulting in a question of what class of a liquid crystals is formed. The system undergoes a clear first-order phase transition, indicating that no phase segregation takes place; i.e., both short and long oligomers are ordered and undergo a phase transition simultaneously. In parallel, our studies have shown that the short oligomers form an isotropic liquid and the longer polymers exhibit a gel phase, which is discussed elsewhere.<sup>27</sup> The formation of a liquid crystalline phase occurs only when short chains are added to longer chains; thus, we consider the system as lyotropic in nature, where the short chains that do not exhibit liquid crystalline behavior are serving as solvent.

The phase diagrams have been constructed primarily from polarized optical microscopic<sup>24</sup> and DSC data. Because of the semifluorinated nature of the phases, shear had to be applied in order to observe birefringence textures. The decay of the birefringence with time provided insight into the molecular structure of the polymer as will be discussed in that context. NMR has been utilized to confirm the inherent order of the phases and to follow the dynamics of the different parts of the molecule.<sup>25,26</sup> Small and wide-angle X-ray scattering revealed the detailed structure of this novel liquid crystal.

**Optical Microscopy: Bulk and Interfacial Characteristics.** Polarized optical microscopy detects the birefringence resulting from the anisotropy of the refractive indices  $\Delta n = n_{\parallel} - n_{\perp}$ , where  $n_{\parallel}$  and  $n_{\perp}$  are the parallel and the perpendicular components of the refractive index  $n$ , with respect to the director of the mesophase.<sup>24</sup> Further characterization of the nature of the phase can be obtained from the observed patterns due to characteristic defects in the LC orientation. Polarized optical microscopy images of a thin sample of branched oligomers ( $M_n = 2240$  and  $M_n/M_w$  of 1.74), captured at room temperature, are shown in Figure 2, parts a and b. The samples were heated to the isotropic phase in order to eliminate thermal history, and cooled to the desired temperature. Figure 2a introduces a dark image of what appears to be a fluid. At the grain boundaries however, small anisotropic domains are

observed. These suggest that the system exhibits some degree of ordering. Very mild shear (e.g., merely touching the top cover slide) resulted in the appearance of clear birefringence textures, shown in Figure 2b. These textures are attributed to the liquid crystalline nature of the sample. The appearance of birefringence following shear may be either a consequence of shear-aligned polymer or a result of an inherently ordered homeotropic LC. Further studies by NMR and X-ray confirmed that the decay behavior is the result of homeotropically aligned LC as will be further discussed. For homeotropic liquid crystals, the director is perpendicular to glass surfaces so the sample appears dark under polarized optical microscopy. When shear is applied, the director changes orientation, allowing the passage of light, and distinct LC textures can be observed. The temperature at which shear did not induce any birefringence corresponds to the order–disorder transition temperature (ODT). The transition into the gel phase has been characterized by optical microscopy following the formation of domains with distinct sharp boundaries, which are characteristic of low dimensional solids and oriented gels. Further confirmation of the ODT was obtained from NMR analysis.

Several groups<sup>19,20,23</sup> have demonstrated the effect of low surface energy on homeotropic alignment. The texture, observed under shear, is the result of the deformation of the director. When the surface interactions are stronger than the elastic modulus, it relaxes back to an initial homeotropic alignment after the perturbation is released. Consequently, the decay of texture is observed. The time that the director takes to relax back to its initial state is defined as the “relaxation time ( $\tau$ )”. The relaxation behavior relies on both the strength of surface interactions and the intrinsic properties of the LC, including its viscoelasticity. In general the relaxation time is inversely proportional to the viscosity ( $\eta$ ) and depends on the molecular shape (spherical cylindrical etc.). Relaxation times of the birefringence textures have been studied as a function of increasing the average molecular weight. The results are summarized in Figure 3, parts a–c. A schematic representation of the experiment is shown in Figure 3a. The samples were encapsulated between two microscope slides. Shear was applied by moving the top slide ca. 3 mm with minimal load. In these experiments, the relaxation time  $\tau$  is defined as the time interval between

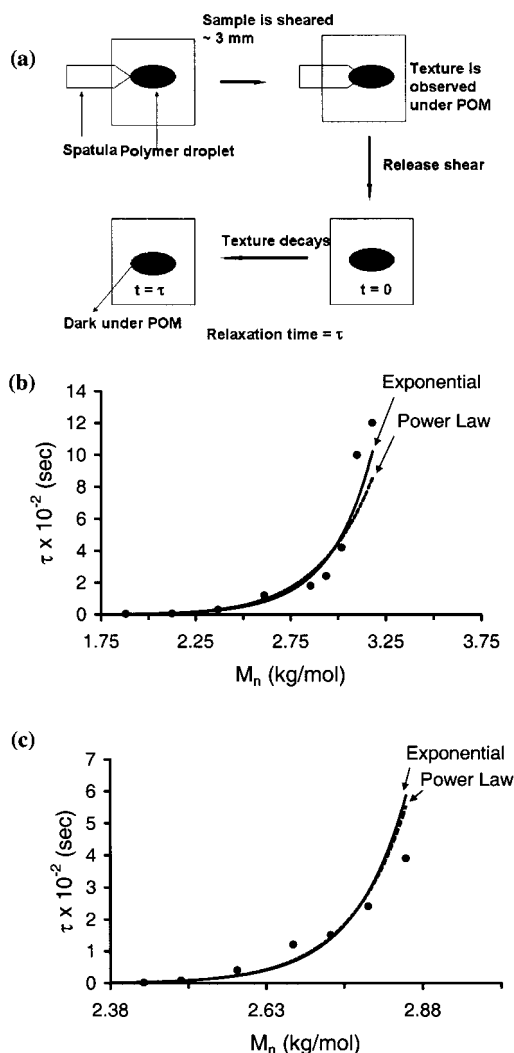


**Figure 3.** The relaxation time ( $\tau$ ) of the birefringence texture as a function of number average molecular weight ( $M_n$ ). Part a corresponds to the experimental setup, b, to the relaxation times for branched polymer, and c to the linear polymer. The solid and dash lines represent the best fits to exponential and power laws, respectively. Relaxation time vs  $M_n$  for branched [exponential yields  $y = 0.0071e^{3.85x}$  and  $R^2 = 0.97$ ; power law yields  $y = 0.0349x^{8.96}$  and  $R^2 = 0.94$ ] for linear [exponential yields  $y = 1E-12e^{11.89x}$  and  $R^2 = 0.97$ ; power law:  $y = 6E-12x^{30.67}$  and  $R^2 = 0.97$ ].

release of the cover slide, and the time birefringence has fully decayed. The relaxation time as a function of  $M_n$  is plotted in Figure 3 for the branched (part b) and linear (part c) samples, respectively. The solid and dashed lines correspond to the best fits to exponential and power law equations, respectively. For a linear polymer,  $\eta \propto aM^\nu$ , and for a weakly cross-linked or branched polymer  $\eta \propto be^{\alpha M}$  where  $a$ ,  $b$ ,  $\alpha$ , and  $\nu$  are the constants.<sup>28</sup> As shown in Figure 3b, the relaxation time is exponential with polymerization time. When branching was chemically blocked, the data are neither pure exponential nor a power law. GPC data combined with the optical microscopy, indicate that the branching was only partially blocked. For the exponential fit, the value of  $\alpha$  for branched systems is on the order of 3.85 while it is 11.89 for the sample, which appears linear by GPC (see figure caption).

The intensity of the birefringence was found to vary slightly with the initial application of a normal load as expected. However the shape of the curves, i.e., expo-

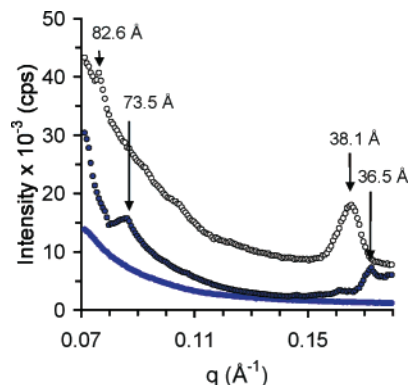


**Figure 4.** SAXS profiles of branched oligomers (top)  $M_n = 2240$ ,  $M_n/M_w = 1.74$  (middle)  $M_n = 1490$ ,  $M_n/M_w = 1.34$ , and (bottom) monomer ( $M_n = 300$ ). Each sample was melted on the sample holder and then scanned overnight at room temperature. Momentum transfer  $q$  is defined as:  $q = 4\pi(\sin \theta)/\lambda$  where  $\theta$  = incident angle and  $\lambda$  = wavelength.

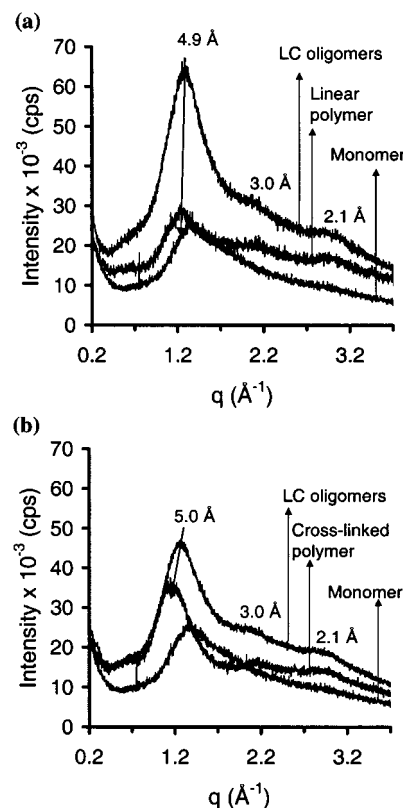


**Figure 5.** WAXD profiles of linear (a) and branched (b) polymers at room temperature. Each sample was melted on sample holder. For the linear system LC oligomers: ( $M_n = 1900$  and linear polymer  $M_n = 6390$ ); For the branched system LC oligomers:  $M_n = 1490$ , branched polymer (insoluble in THF).

nential or power law, does not change. While there are quantitative, relaxation measurements they are consistent with the GPC data. The optical microscopy provided bulk and interfacial characteristics. Further structural information was obtained from X-ray studies.

**Structure by SAXS and WAXD.** Measurements were carried out on the monomer and on different lyotropic mixtures. Representative SAXS and WAXD patterns are shown in Figures 4 and 5, respectively. The SAXS pattern for a relative long branched chain ( $M_n = 2240$  with  $M_n/M_w = M_w = 1.74$ ), consists of two clear peaks at  $q = 0.077$  and  $0.16 \text{ \AA}^{-1}$  corresponding to

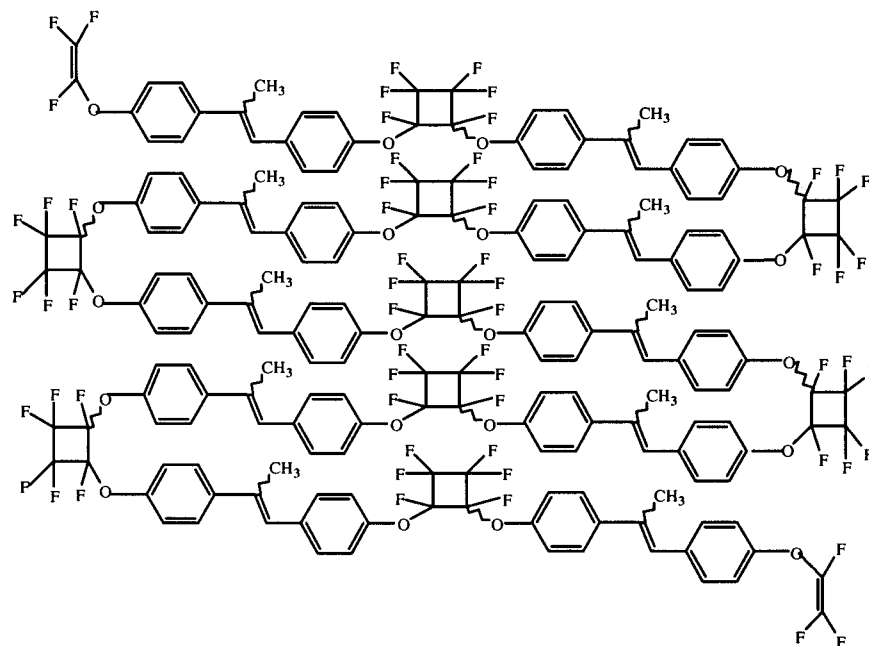


**Figure 6.** Schematic representing the lamellar structure of LC PFCB.

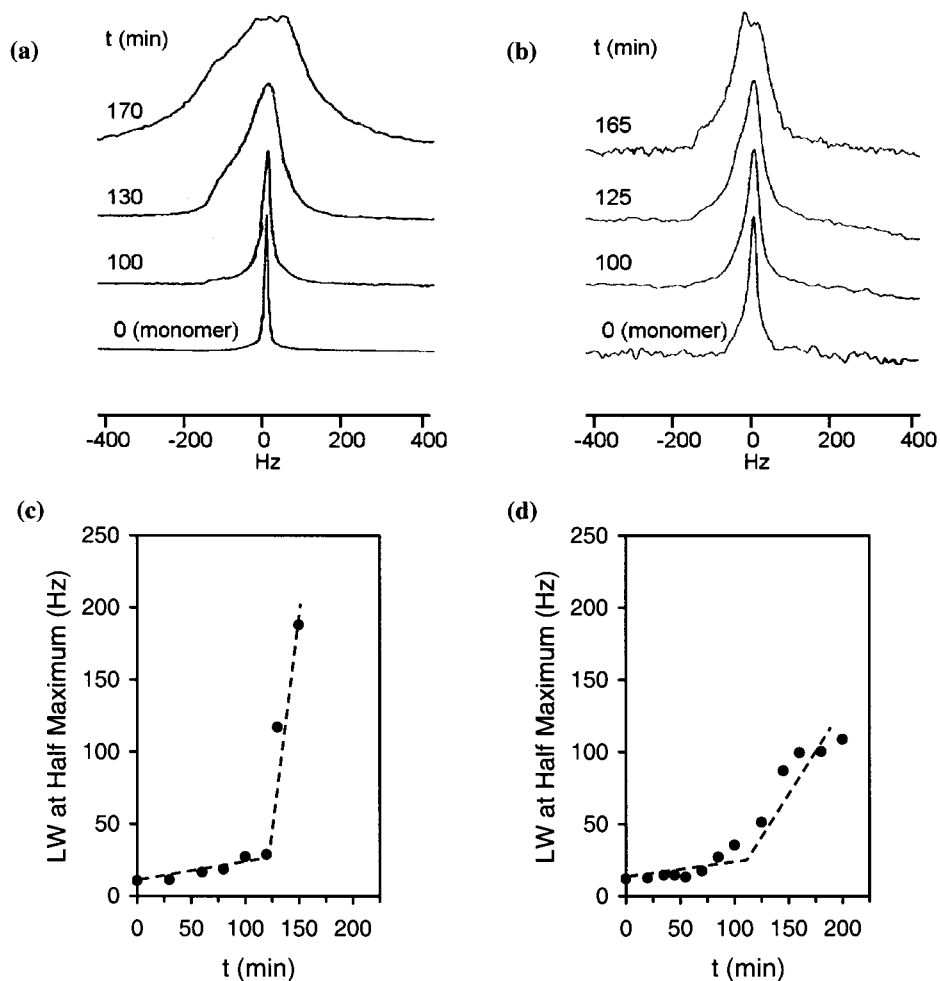


**Figure 7.**  $^2\text{H}$  NMR spectra of  $\sim 1$  wt % deuterated cyclohexane dissolved in the polymers. Samples were heated in the NMR tube and cooled inside the NMR magnet. Spectra were taken at room temperature as a function of polymerization time ( $t$ ). a and b correspond to the spectra of the linear and branched systems respectively, c and d represent that for the linear (c) and for the branched system (d). Line widths (LW) at half-height maximum of each spectrum were plotted vs  $t$  in order to observe the formation of mesophase. Dashed lines in plots c and d are guiding lines.

$\sim 80$  and  $\sim 38.0$  Å. These lines exhibit a ratio of approximately 1:2, suggesting lamellar packing.<sup>29</sup> For the

shorter chains ( $M_n = 1490$  and  $M_w/M_n = 1.34$ ), a broad line is observed at  $q = 0.088$  and  $0.17$  Å<sup>-1</sup> corresponding

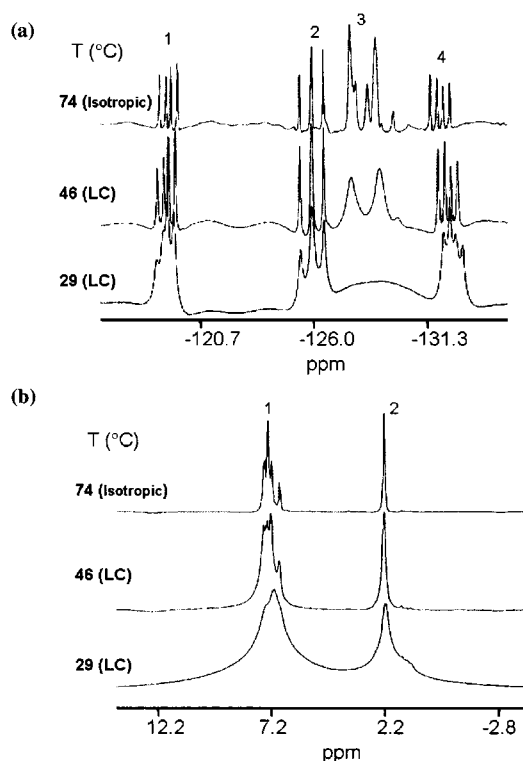


**Figure 8.** (a)  $^{19}\text{F}$  and (b)  $^1\text{H}$  NMR spectra of branched oligomers ( $M_n = 2240$ ,  $M_n/M_w = 1.74$ ) upon heating. Neat oligomers were heated inside the NMR magnet, and then spectra were taken with the increasing temperature. For  $^{19}\text{F}$  signals at positions 1, 2, 4 = trifluorovinyl end group while signals at position 3 = PFCB group. For  $^1\text{H}$ : Signals at positions 1 = aromatic and signal at positions 2 = methyl (see Scheme 1). At liquid crystalline phase (46, 29 °C), peaks broaden due to nonaveraged dipolar interaction.

to 73.4 and 36.5 Å, with a ratio of 1:2. No long-range periodicity was observed for the monomer ( $M_n = 300$ ).

The high  $q$  measurements are shown in Figure 5. The monomer, which is an isotropic liquid, exhibits a broad liquid–liquid correlation peak centered at  $\sim 4.5$  Å. Upon polymerization, this peak narrows, and further lines at 3 and 2 Å, appear. The peak at 5 Å is slightly shifting with molecular weight, where the peaks at 3 and 2 Å are independent of chain length. These correspond to internal molecular internal distances. The broad background, which underlines the pattern, corresponds to the smaller oligomers, which serve as a solvent for this lyotropic system. A schematic model for the structure within the layers is given in Figure 6. The 5 Å line is consistent with stacking of the fluorinated PFCB rings, as we have found in other similar crystalline derivatives. This together with the distinct changes in its line width upon transitions between the isotropic and LC phase suggests that this line corresponds to an interlayer distance. The  $\sim 80$  Å layer width includes the organized chains and the smaller chains that serve as solvent. Further small angle X-ray studies are currently underway to determine the factors, which affect this periodicity.

**NMR Studies.** NMR measurements were carried out on a deuterated probe, cyclohexane- $d_{12}$ , as well as on the proton and fluorine nuclei on the polymeric backbone. Using a deuterated probe to study the phase diagram of a liquid crystalline material is a well-established technique.<sup>25,26</sup> In most protonated LCs, the ordering pattern of a guest molecule dissolved in the

LC media reflects the trend of the order in the LC phase itself.

In this experiment, the deuterated cyclohexane was used as a probe molecule. Its spectrum has been studied in different LC solvents. Samples of different branching degrees and molecular weight were heated to the isotropic phase and were cooled in the magnetic field. The NMR spectra were recorded at different temperatures. In the isotropic phase, the spectrum consists of a single line. Further cooling leads to a powder pattern over all the temperature and LC concentration range. The room temperature  $^2\text{H}$  NMR spectra as a function of polymerization time are presented in Figure 7, parts a and b, for the linear and branched materials, respectively. In both systems the powder pattern does not change after several hours in the magnetic field. This suggests that the sample does not orient in the magnetic field. The probe measurements have clearly indicated that the birefringence patterns correspond to an anisotropic system. The plots of the line width as a function of polymerization time at a given temperature exhibit a discontinuity as shown in Figure 7, parts c and d. The broadening of the line corresponds to the phase transition into the LC phase.

Further NMR measurements were carried out on the mesogenic molecule itself. Figure 8, parts a and b, shows  $^{19}\text{F}$  and  $^1\text{H}$  NMR spectra, respectively, as a function of temperature for branched oligomers ( $M_n = 2240$ ,  $M_n/M_w = 1.74$ ). Three distinct dd patterns (Figure 8a) at positions 1, 2, and 4 correspond to trifluorovinyl end groups while the multiplet at position 3 represent the six nonequivalent fluorine atoms on each *cis*- and *trans*-1,2-disubstituted cyclobutane linkage.<sup>1,2</sup>  $^1\text{H}$  NMR spectra (Figure 8b) exhibit the aromatic proton signals (with olefinic proton singlet shoulder) at position 1 and the methyl proton signals at position 2. In the mesophase (29, 46 °C), all peaks are broadened due to none averaged dipolar interactions.<sup>25</sup> The spectra in the isotropic phase are narrow and well defined (74 °C). Upon cooling into the mesophase, both the  $^{19}\text{F}$  and  $^1\text{H}$  spectra broaden significantly, as expected. The degree of broadening of different components in the spectrum reflects a different degree of motion and order of different parts of the molecule. While at temperatures where the lines of the end vinyl group in the fluorine spectra (Figure 8a, groups 1, 3, and 4), are still narrow, the lines that correspond to the PFCB broaden significantly. Similarly, the spectra of aromatic protons broaden (Figure 8b) at higher temperatures than the spectrum of the protons on the methyl group. The protons of the methyl group consist of one line. Upon cooling, the line slightly broadens, but since the other nuclei with large dipolar couplings are not adjacent to the methyl groups, the broadening is rather mild and allows the detection of the chemical shift anisotropy.<sup>25</sup> The chemical shift anisotropy,  $\Delta\delta$ , is a measure of the order parameter in the system.

The values of  $\Delta\delta$  for the methyl group protons are plotted as a function of temperature in Figure 9. To quantitatively calculate the order parameter from the chemical shift anisotropy, one should be able to measure the diamagnetic susceptibility,  $\Delta\chi$ , and obtain the components of the chemical shift anisotropy tensor for  $S = 1$ . Since this lyotropic system did not orient in a magnetic field we do not have the value for  $\Delta\chi$ . Moreover, the value for the chemical shift tensor for this group is unknown. From Figure 9, we can qualitatively

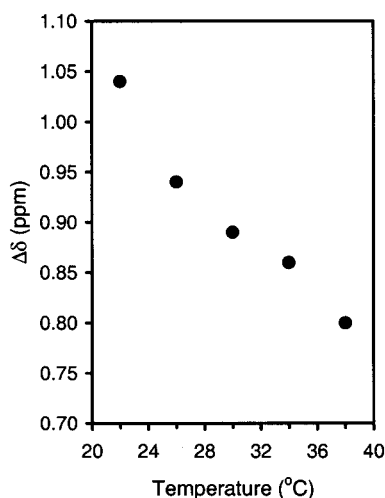
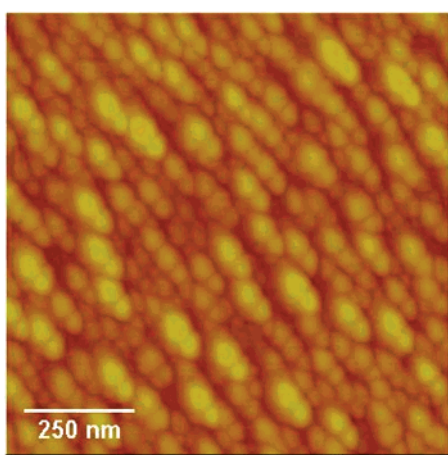


**Figure 9.** Anisotropic chemical shift ( $\Delta\delta = \delta_{\perp} - \delta_{\parallel}$ ) of the methyl group as a function of temperature.



2D spectrum from FT

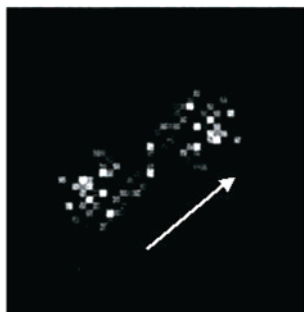


**Figure 10.** (Top) Structure of LC branched oligomers on glass surface revealed by tapping mode AFM. Sample ( $M_n = 2240$ ) was dissolved in toluene. The droplet of solution on glass slide was evaporated at room temperature in a laminar hood. The LC film coated on glass was scanned under ambient condition. (Bottom) Fourier transform (FT) of the image showing periodicity in the orthogonal direction (arrow) with the average distance  $\sim 50$  nm. Set point = 1.654 V, and scan size =  $1 \mu\text{m}$ .

deduce that the order parameter increased with decreasing temperature. No singularities are observed within the LC regime.

The NMR results have clearly shown that inherent ordering in these lyotropic lamellar systems exists. In addition, we can detect a clear difference in the order and dynamics of the PFCB ring, the aromatic groups and the aliphatic groups. While the PFCB moiety and

the aromatic group are locked in the structure, the methyl and the end groups are much freer to move. The X-ray and NMR data provided information on structure and dynamics of the new PLC on an angstrom to a tenth of an angstrom scale. The optical microscopy provided information on the micrometer scale. Further studies were carried out on the nanometer scale using AFM.

**Nanometer Scale Surface Structure.** When thin films less than  $1 \mu\text{m}$  were cast on a glass support, long-range order, which consisted of nanometer scale bundles, was observed. Figure 10 introduces a tapping mode AFM image. Samples were prepared by evaporating solution of LC polymer on glass slide, without shear. The Fourier transform of the image consists of a peak centered at 50 nm. Further studies are currently on the way to further understand the origin of this nanoscale ordering.

## Conclusions

The structure and dynamics of bulk and thin films of a novel semi fluorinated lyotropic mesophase have been studied. In thin films, between glass slides, the PLC exhibits homeotropic behavior with characteristic decay time varying between 1 and 1200 s, depending on the molecular weight. The homeotropic characteristics are attributed to the low surface energy of the PFCB group. The bulk mesophases of both linear and branched oligomers consist of lamellar organized structures, immersed in smaller oligomers. The order of the phases increases with decreasing temperature, where different parts of the molecule exhibit different levels of order. We have observed order on several length scales: on the angstrom level, the structure within the layer was detected, and on the 100 Å level, we observed the layer spacing. When the PLC is cast into thin films, further order on the nanometer length scale has been observed by AFM.

**Acknowledgment.** The authors thank Clemson University (start-up funds for D.W.S. and D.P.), The Dow Chemical Company, and a 3M Pre-tenured Faculty Award (D.W.S.) for financial support. We also thank Mettler-Toledo for the donation of a DSC820 system to Clemson University, the Thai Government for a Graduate Fellowship (R.T.), and H. Boone (Dow) for kind assistance.

## References and Notes

- (1) Smith, D. W., Jr.; Boone, H. W.; Traiphol, R.; Shah, H. V.; Perahia, D. *Macromolecules* **2000**, *33*, 1126.
- (2) Smith, D. W., Jr.; Babb, A. D.; Shah, V. H.; Hoeglund, A.; Traiphol, R.; Perahia, D.; Boone, H. W.; Langhoff, C.; Radler, M. *J. Fluorine Chem.* **2000**, *104*, 109.
- (3) Lau, W. Y.; Burns, C. M. *J. Polym. Sci. Polym. Phys. Ed.* **1974**, *12*, 431.
- (4) Wu, S. H., *Polymer Interfaces and Adhesion*; Marcel Dekker: New York, 1982.
- (5) For a recent review, see: *Modern Fluoropolymers*; Scheirs, J., Ed.; Wiley: New York, 1997.
- (6) Perutz, S.; Wang, J.; Kramer, E. J.; Ober, C. K.; Ellis, K. *Macromolecules* **1998**, *31*, 4272.
- (7) Marczuk, P.; Lang, P. *Macromolecules* **1998**, *31*, 9013.
- (8) Wang, J.; Ober, C. K. *Macromolecules* **1997**, *30*, 7560.
- (9) Fuhrmann, Th.; Hosse, M.; Lieker, I.; Rubner, J.; Stracke, A.; Wendorff, J. H. *Liq. Cryst.* **1999**, *26*, 779.
- (10) Hird, M.; Toyne, K. J. *Mol. Cryst. Cryst. Sci. Technol., Sect. A* **1998**, *323*, 1.
- (11) Yang, X.; Abe, K.; Kato, R.; Yano, S.; Kato, T.; Miyazawa, K.; Takeuchi, H. *Liq. Cryst.* **1998**, *25*, 639.
- (12) Bryan-Brown, G. P.; Wood, E. L.; Sage, I. C. *Nature* **1999**, *399*, 338.

- (13) Kanie, K.; Tanaka, Y.; Takehara, S.; Hiyama, T. *Chem. Lett.* **1998**, 1169.
- (14) Wang, J.; Ober, C. K. *Liq. Cryst.* **1999**, 26, 637.
- (15) Shiota, A.; Ober, C. K. *Macromolecules* **1997**, 30, 4278.
- (16) Benicewicz, B. C.; Smith, M. E.; Earls, J. D.; Priester, R. D., Jr.; Setz, S. M.; Duran, R. S.; Douglas, E. P. *Macromolecules* **1998**, 31, 4730.
- (17) Percec, V.; Kawasumi, M. *Macromolecules* **1993**, 26, 3663.
- (18) Basturk, N. *Liq. Cryst.* **1993**, 14, 525.
- (19) Bates, F. S. *Science* **1991**, 251, 898.
- (20) Watanabe, R.; Nakano, T.; Satoh, T.; Hatoh, H.; Ohki, Y. *Jpn. J. Appl. Phys.* **1987**, 26, 373.
- (21) Seo, D.; Kobayashi, S. *Jpn. J. Appl. Phys.* **1995**, 34, 786.
- (22) Dennis, J. T.; Vogel, V. *J. Appl. Phys.* **1998**, 83, 5195.
- (23) Shahidzadeh, N.; Merdas, A.; Urbach, W.; Arefi-Khonsari, F.; Tatoulian, M.; Amouroux, J. *Langmuir* **1998**, 14, 6594.
- (24) Hartshorne, N. H.; Stuart, A. In *Crystals and the polarizing Microscope*; Ernold, E., Ed.; Elsevier Science: Amsterdam, 1970, and references therein.
- (25) Emsley, J. W. *Nuclear Magnetic Resonance of Liquid Crystals*; D. Reidel Publishing Company: Dordrecht, The Netherlands, 1985.
- (26) Terzis, A. F.; Poon, C.; Samulski, E. T.; Luz, Z.; Poupko, R.; Zimmermann, H.; Muller, K.; Toriumi, H.; Photinos, D. J. *J. Am. Chem. Soc.* **1996**, 118, 2226.
- (27) Traiphol R.; Felcher G.; Smith, D. W., Jr.; Perahia D. Manuscript in preparation.
- (28) De Gennes, P.-G. *Scaling concepts in Polymer Physics*; Cornell University Press: Ithaca, NY, 1979.
- (29) Note that the low  $q$  data are broad and superimposed on top of the main beam; thus, the errors in assigning the peak position are relatively large, allowing the difference to be between 80 and 76 Å. Note that an empty cell has been run for each measurement.

MA0017891